Far East Journal of Mathematical Sciences (FJMS)
© 2018 Pushpa Publishing House, Allahabad, India
http://www.pphmj.com
http://dx.doi.org/10.17654/MS103111769
Volume 103, Number 11, 2018, Pages 1769-1788 **ISSN: 0972-0871**

RECOGNITION OF FACE IMAGES UNDER VARYING HEAD-POSES USING FFT-PCA/SVD ALGORITHM

Richard K. Avuglah[1], Louis Asiedu[2,*], Ezekiel N. N. Nortey[3] and Favour N. Yirenkyi[4]

[1,4]Department of Mathematics
Kwame Nkrumah University of Science and Technology
Kumasi, Ghana

[2,3]Department of Statistics
School of Physical and Mathematical Sciences
College of Basic and Applied Sciences
University of Ghana
Legon-Accra, Ghana

Abstract

The human brain has the inborn characteristics to distinguish between faces. The human brain has particular nerve cells for responding to local features of a scene, such as edges, angles, lines or movements. Automated intelligent systems have been developed to mimic this skill inherent in human beings. These systems extract meaningful features from an image, put them into useful representations and classify them. Amidst these achievements is the challenge of recognizing face images under varying constraints. This study assessed the performance of principal component analysis with singular value decomposition

Received: September 16, 2017; Accepted: December 21, 2017
2010 Mathematics Subject Classification: 62H25, 62H35.
Keywords and phrases: fast Fourier transform, repeated measures design, principal component analysis, singular value decomposition, face recognition algorithm.

*Corresponding author

using fast Fourier transform for preprocessing (FFT-PCA/SVD) face recognition algorithm under specified angular constraints (4°, 8°, 12°, 16°, 20°, 24°, 28° and 32°). Ten face images from 10 subjects captured under straight-pose (0°) were used for training in the face recognition module. Eighty face images from 10 subjects captured under the specified constraints were used for testing. The study adopted the repeated measures design to ascertain whether statistically significant differences exist in the average recognition distance of the various angular constraints from their straight-pose when the FFT-PCA/SVD is used for recognition. The results of the study revealed that statistically significant differences exist in average recognition between all head-poses except those that are at 4° or less apart. The study also found that FFT-PCA/SVD has a high average recognition rate of 92.5% with corresponding error rate of 7.5%. The study algorithm (FFT-PCA/SVD) recognizes perfectly (100% recognition rate) head-poses that are 24° and below. FFT-PCA/SVD is therefore recommended for recognition of face images under varying head-poses.

1. Introduction

Humans are endowed with an ability to recognize faces. This recognition ability is stress-free among humans. According to Turk and Pentland [11], even though the capacity to deduce the astuteness from facial expression is doubtful, human beings have outstanding capability to recognize faces. Automatic face recognition has to do with extracting expressive features from an image, forming useful representation and performing some kind of identification from them (Wagner [12]).

According to Samal and Starovoitov [9], face recognition system can be classified into two categories. One is a system that checks to see if a person belongs to a restricted group. Such systems are usually used in access control. The other is a system that identifies a person from a large database by photo search.

It was established by Turk and Pentland [11] that the performance of face recognition algorithms is restricted by constrained environments.

Morrigan et al. [8] reported that face recognition models are sensitive to variation based on an individual image pose position.

Asiedu et al. [2] statistically evaluated the performance of three face recognition algorithms under varying facial expressions. In their study, FFT-PCA/SVD was adjudged the most efficient and consistent recognition algorithm. However, they admitted that their result was limited to varying facial expressions and the best adjudged algorithm could be challenged under different constraints.

Having been established by Asiedu et al. [2] that FFT-PCA/SVD algorithm performs comparatively better under variable facial expressions, it would be worthwhile to assess the performance of the aforementioned algorithm under angular constraints. This study therefore seeks to evaluate the performance of FFT-PCA/SVD algorithm under angular constraints.

2. Materials and Methods

This study adopted a secondary database which was extracted from the Massachusetts Institute of Technology (MIT) (2003-2005) database. Subjects from the MIT database have been captured under various angular poses (4°, 8°, 12°, 16°, 20°, 24°, 28° and 32°). Ten of the images along neutral poses (0°) are trained into the database whereas the remaining eighty images collected, subject to angular constraints (4°, 8°, 12°, 16°, 20°, 24°, 28° and 32°), are captured into the test image database. The images captured into the test image database are known as the test images and are used for testing the recognition algorithm. To keep the data uniform, captured images were digitalized into gray-scale precision and resized into 100×100 dimensions and the data types changed into double precision for preprocessing.

The FFT-PCA/SVD algorithm is used to train the image database. During the training phase, unique face features of the training set are extracted and stored in memory. At the testing phase, a new face image is put into the face recognition module and its features are calculated according to a

specified algorithm's procedure. The extracted features are compared through computation of the Euclidean distances. A maximum difference signifies a poor match while a minimum difference indicates a close match.

2.1. Data acquisition

As stated earlier, the study adopted Massachusetts Institute of Technology (MIT) database (2003-2005) to benchmark the face recognition algorithm (FFT-PCA/SVD). Face image subjects in the database were captured under some specified angular constraints. Specifically, the faces were rotated in depth from 0° to 32° in 4° increments.

All face images were normalized and digitized into gray-scale precision and resized into uniform dimension (100×100). This made computation easy. Figure 1 shows the original face images of the 10 individuals in the adopted database.

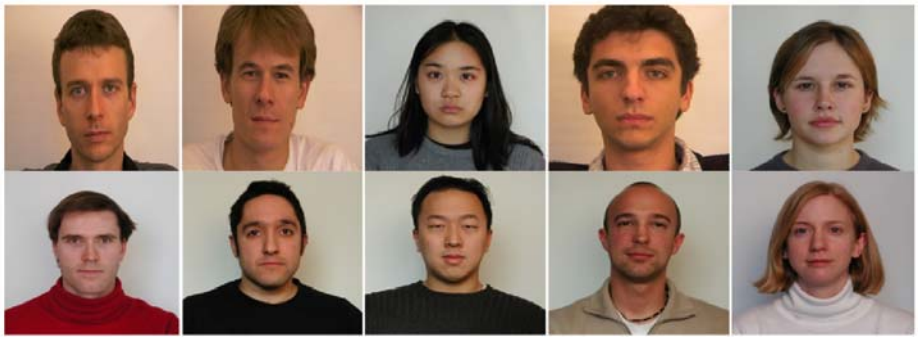

Figure 1. Original images generated for all ten subjects: (Weyrauch et al. [13]).

Ten images from 10 individuals under the straight pose (0°) were captured into the train image database for training and feature extraction and knowledge creation. Figure 2 shows the 10 images used for the train image database.

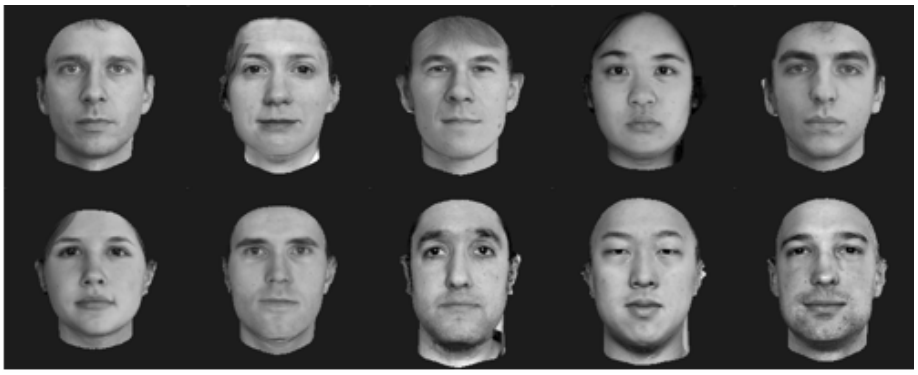

Figure 2. Train image database: (Weyrauch et al. [13]).

Eighty images from 10 individuals under the specified angular constraints (4°, 8°, 12°, 16°, 20°, 24°, 28° and 32°) were captured into the test image database for testing and recognition. Figure 3 shows captured images under the specified constraints for 3 individuals.

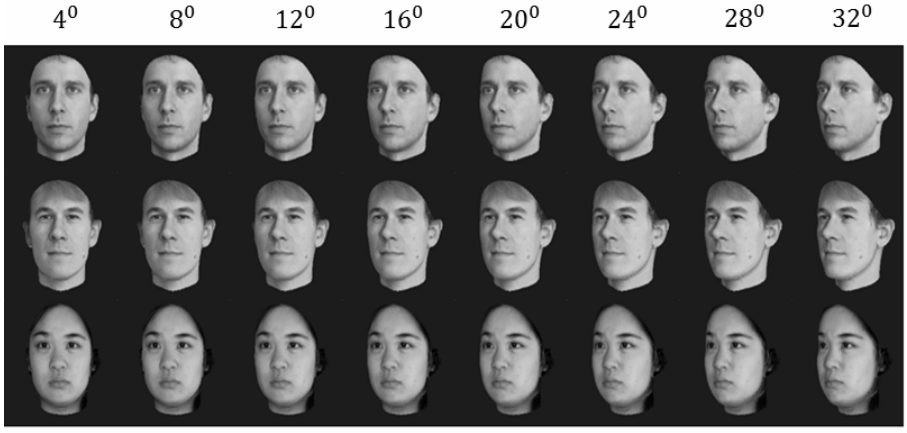

Figure 3. Sample of test image database: (Weyrauch et al. [13]).

Face images were passed to the adopted recognition model as inputs. These inputs were converted into working compatible formats (resizing into uniform dimensions). The passed data were digitized into gray-scale double precision. The fast Fourier transform mechanism was adopted during the face image preprocessing stage. This, according to Asiedu et al. [2],

helps reduce the noise and makes the estimation process easier and well conditioned.

The face images were then passed through the extraction unit in the recognition system for extraction of unique face features. The obtained features were sent to the classifier unit for classification. Here, created knowledge is stored in the system's memory for recognition purposes.

When a test face (image captured under angular constraints) was introduced, its data information were calculated along the above description and compared to the trained information stored in memory. A minimum Euclidean distance was seen as a close match and vice versa. Figure 4 shows the research design.

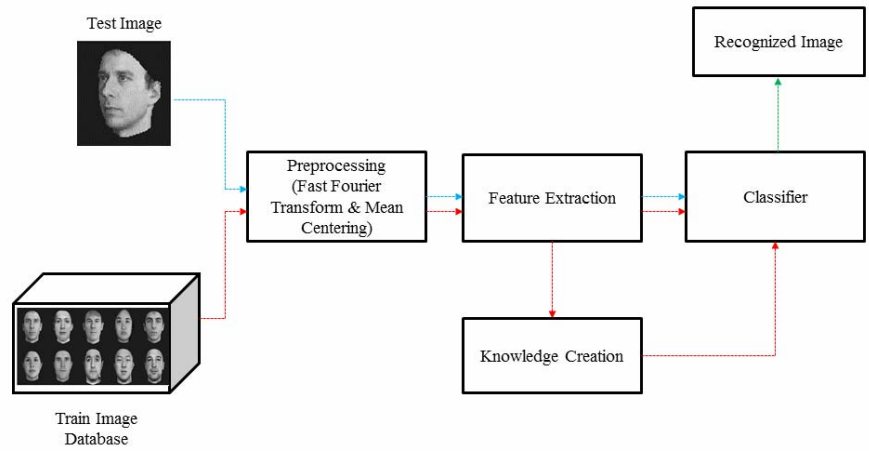

Figure 4. Research design.

2.2. Preprocessing of face images

Preprocessing stage is an effective way of removing noise and suppressing unwanted distortion of image feature for further processing. It helps to significantly increase the reliability and performance of a recognition system. It also helps to reduce the noise level, making the estimation process simpler and better conditioned (Asiedu et al. [1]). The principle of preprocessing images helps to enhance the quality of an image in order to improve the performance of the face recognition algorithm. The

adopted preprocessing mechanisms in the study were mean centering and fast Fourier transform.

2.3. Mean centering

Now define an image matrix $\mathbf{A}_j$ as

$$\mathbf{A}_j = (a_{jik}); \quad i, k = 1, 2, ..., p; \; j = 1, 2, ..., n$$

$$= (\mathbf{a}_{j1}, \mathbf{a}_{j2}, ..., \mathbf{a}_{jp}),$$

where $\mathbf{a}_{jk} = (a_{j1k}, a_{j2k}, ..., a_{jpk})^T$.

$$\mathbf{X}_j = (\mathbf{a}_{j1}^T, \mathbf{a}_{j2}^T, ..., \mathbf{a}_{jp}^T)^T, \tag{2.1}$$

where

$p =$ the order of the image matrix,

$n =$ the number of images to be trained.

From equation (2.1), suppose $\mathbf{X}_j$ is a column vector of dimension N given by

$$\mathbf{X}_j = (X_{ji})_{N\times 1}, \tag{2.2}$$

where X_{ji} replaces the a_{jik} position-wise. The preprocessing steps are based on the sample $X = (\mathbf{X}_1, \mathbf{X}_2, ..., \mathbf{X}_n)$, whose elements are the vectorised form of the individual images in the study.

The mean centering preprocessing mechanism is performed by subtracting the mean image from the individual images under study. The mean is given by

$$\bar{\mathbf{a}}_j = E(\mathbf{X}_j), \quad j = 1, 2, ..., n$$

$$\bar{\mathbf{a}}_j = \frac{1}{N}\sum_{i=1}^{N} X_{ji}$$

$$= \frac{1}{N}\sum_{i=1}^{p}\sum_{k=1}^{p} \mathbf{a}_{jik} \quad (j = 1, 2, 3, ..., n), \tag{2.3}$$

where $N = (p \times p)$, length (= rows of image × columns of image) of the image data $\mathbf{X}_j$.

Define $\overline{\mathbf{X}}_j$ as a constant vector of order $(p \times p)$ with all elements same as $\bar{\mathbf{a}}_j$ $(j = 1, 2, ..., n)$ (Asiedu et al. [1]).

The mean centered matrix is denoted by $\mathbf{W} = (\mathbf{w}_1, \mathbf{w}_2, \mathbf{w}_3, ..., \mathbf{w}_n)$, where

$$\mathbf{w}_j = \mathbf{X}_j - \overline{\mathbf{X}}_j. \tag{2.4}$$

2.3.1. Fast Fourier transform

Fast Fourier transform (FFT) can be used as a noise reduction mechanism during image preprocessing. The FFT is an efficient computation of discrete Fourier transform (DFT) and its inverse (IDFT). The FFT algorithm reduces the computational burden to $O(N\log N)$ arithmetic operations (Glynn [4]). FFT is preferred to DFT when working with large data because it is computationally faster than DFT. FFT gets its speed by decreasing the number of calculations needed to analyze an image data.

The first stage in the execution of FFT during image preprocessing is to compute the discrete Fourier transform. The DFT of a column vector $\mathbf{a}_{jk}$ is represented mathematically as

$$\mathbf{a}^*_{jk} = DFT\{\mathbf{a}_{jk}\} = \sum\nolimits_{r=0}^{p-1} \mathbf{a}_{jk} e^{-i(2\pi sr/p)}, \tag{2.5}$$

where $s = 0, 1, ..., p-1$, $j = 1, 2, ..., n$. $\mathbf{a}_{jk}$ is the kth column of the image matrix $\mathbf{A}_j$.

The default noise in face images is mostly the Gaussian noise because of illumination variations. This study therefore adopted a Gaussian filter for de-noising the face images after the discrete Fourier transformation.

After filtering, the inverse discrete Fourier transformations (IDFTs) were performed to reconstruct images into their original forms. The inverse

discrete Fourier transform (IDFT) is given by

$$\mathbf{a}_{jk} = IDFT\{\mathbf{a}^*_{jk}\} = \frac{1}{p}\sum_{r=0}^{p-1}\mathbf{a}^*_{jk}e^{i(2\pi sr/p)},$$

$$s = 0, 1, ..., p-1, \; j = 1, 2, ..., n. \tag{2.6}$$

After the inverse transformation, the imaginary components were discarded as noise and the real components were extracted for the feature extraction stage. Figure 5 shows the stages in FFT preprocessing of an image.

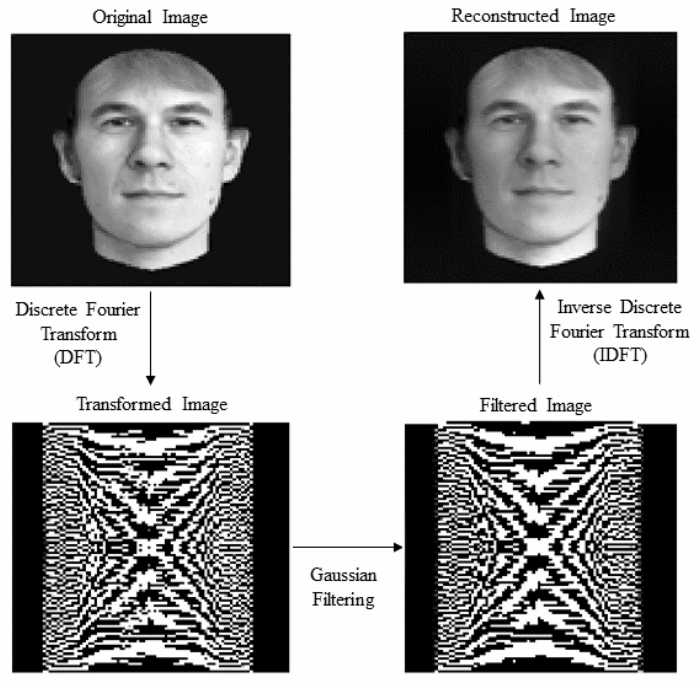

Figure 5. FFT preprocessing cycle.

2.4. Singular value decomposition (SVD)

SVD plays a significant role in routine statistical operations and in structures for data compression founded on approximating a given matrix dataset with another of lower rank. It also plays a central role in the theory of unitary invariant norms. Many modern computational algorithms are based

on SVD because the problem of computing the eigenvalues of a general matrix (like the problem of computing the eigenvalues of a Hermitian matrix) is well-conditioned (Horn and Johnson [5]).

The SVD is related to the familiar theory of diagonalizing a symmetric matrix. If **B** is a symmetric real $r \times r$ matrix, then there exist an orthogonal matrix **U** and a diagonal matrix **S** such that $\mathbf{B} = \mathbf{USU}^T$. The columns of **U** are seen here as the eigenvectors for **B** and they form an orthonormal basis for $\mathbb{R}^r$. The diagonal entries of **S** are the corresponding eigenvalues of **B**.

For an asymmetric matrix **C** of dimension $k \times r$, the SVD transformation takes $\mathbb{R}^r$ to a different space $\mathbb{R}^k$. This is done by decomposing **C** into orthogonal matrices **V**, **U** and a diagonal matrix **S**. The columns of **V** and **U** provide the basis for **C**.

2.5. Principal component analysis (PCA)

Image space is very large and its storage requires reduction of the dimensions of original images using feature extraction methods. One such method for feature extraction is the principal component analysis (PCA). PCA is also referred to as Karhunen-Loéve transformation (Kirby and Sirovich [6]).

According to Shlens [10], PCA computes the most meaningful basis to re-express a noisy garbled dataset. The rationale behind this new basis is to filter out the noise and reveal hidden dynamics in the dataset. That is, PCA extracts the most significant components or those components which are more informative and less redundant, from the original data.

PCA basically rotates the set of points around their mean in order to align with the first few uncorrelated components that carry important information about the data. Much of the variability in the data is accounted for by the first principal component and the remaining variability is taken care of by other components.

2.6. Feature extraction

According to Lajevardi and Hussain [7], feature extraction plays a vital role to reduce the computational cost and promotes the classification results because selecting a low dimensional feature subspace from a bundle of features is very crucial for optimal classification. Incorrect feature selection reduces the performance of face recognition, even though a superlative classifier may be used.

At this stage of the study, unique face identifiers were extracted for recognition. This is done by finding a set of *n* orthonormal vectors $\mathbf{z}_j$ which best describe the distribution of the data. The *r*th vector $\mathbf{z}_r$ is chosen such that

$$\lambda_r = \frac{1}{n}\sum_{j=1}^{n}(\mathbf{z}_j^T\mathbf{w}_j)^2 \tag{2.7}$$

is a maximum subject to the orthonormality constraints

$$\mathbf{z}_l^T\mathbf{z}_r = \delta_{lr} = \begin{cases}1, & l = r,\\ 0, & \text{elsewhere.}\end{cases}$$

The eigenvectors and eigenvalues of the covariance matrix are represented by $\mathbf{z}_r$ and scalars λ_r, respectively,

$$\mathbf{C} = \frac{1}{n}\mathbf{W}\mathbf{W}^T, \tag{2.8}$$

where the mean centered matrix $\mathbf{W} = (\mathbf{w}_1, \mathbf{w}_2, ..., \mathbf{w}_n)$.

The eigenvalues and their corresponding eigenvectors are extracted from singular value decomposition (SVD) of the matrix $\mathbf{C} = \mathbf{U}\mathbf{\Sigma}\mathbf{V}^T$.

This decomposes the covariance matrix **C** into two orthogonal matrices **U** and **V** and a diagonal matrix $\mathbf{\Sigma}$:

$$\mathbf{z}_j = \sum_{j=1}^{n}\mathbf{w}_j\mathbf{u}_j, \tag{2.9}$$

where $\mathbf{u}_j$ is the *j*th column vector of **U**.

From the training set, the principal components are extracted as

$$\gamma_j = \mathbf{z}_j^T(\mathbf{x}_j - \bar{\mathbf{a}}), \tag{2.10}$$

and $\mathbf{\Gamma}^T = [\gamma_1, \gamma_2, ..., \gamma_n]$.

When a new face (test image) is passed through the recognition module, its unique features are extracted as

$$\gamma_j^* = \mathbf{z}_j^T(\mathbf{x}_r - \bar{\mathbf{a}}),$$

and $\mathbf{\Gamma}_r^{*T} = [\gamma_1^*, \gamma_2^*, ..., \gamma_n^*]$.

The recognition distances (Euclidean distances) are computed as

$$\psi = \| \mathbf{\Gamma} - \mathbf{\Gamma}_r^* \|. \tag{2.11}$$

The minimum Euclidean distance $\varepsilon_m = \min[\psi]$ is chosen as the recognition distance.

2.7. Statistical assessment

In this study, 8-variates were collected during the study of algorithm from the Euclidean distance between the various angular constraints (4°, 8°, 12°, 16°, 20°, 24°, 28° and 32°) from their straight-pose (0°) (see Appendix 1.0 for the multivariate dataset).

Define $\mathbf{X}_{jk}$ dataset, $k = 1, 2, ..., p$ and $j = 1, 2, ..., n$. p is the number of constraints excluding the straight pose and n is the number of individuals in the study database.

The repeated measures design was adopted to ascertain whether significant difference exists in the average recognition distance of the various head-poses from their straight pose when the study algorithm is used for recognition. The specified angular constraints (4°, 8°, 12°, 16°, 20°, 24°, 28° and 32°) were seen as treatments. The test is quite sensitive to the assumption of multivariate normality. In violation of the multivariate normality assumption, the non-parametric (distribution-free) counterpart of this test (Friedman's rank sum test) would be adopted.

2.8. Assessing multivariate normality

The repeated measures design is sensitive to multivariate normality assumption. There is no absolutely definitive method for assessing multivariate normality. It is therefore important to perform more than one test to confirm multivariate normality.

2.8.1. Doornik-Hansen multivariate normality test

This study adopted the Doornik-Hansen multivariate normality (DH-MVN) test and confirmed its result with the gamma plot of the data quantiles against the normal quantiles. The Doornik-Hansen test for multivariate normality is based on the skewness and kurtosis of multivariate data that is transformed to ensure independence (Doornik and Hansen [3]). According to Doornik and Hansen [3], the DH test is more powerful than the Shapiro-Wilk test for most tested multivariate distributions.

3. Results and Discussion

The Doornik-Hansen multivariate normality test gave a test statistic value of 11.655 with a corresponding *p*-value of 0.7673. The *p*-value (0.7673) is greater than 0.05 level of significance. Thus, the observed data follow multivariate normal distribution at 5% level of significance.

Figure 6 shows the chi-square plot from the generalized squared distance and the normal quantiles. This plot was used to confirm the result from the Doornik-Hansen multivariate normality test.

It can be seen from Figure 6 that observed data quantiles are aligned close to the line with unit slope. There is no systematic deviation from normality. Also, using the correlation test, the correlation, *r*, value between the observed data quantiles and the normal quantiles is 0.9546. This value (0.9546) is greater than the expected 0.9198 for a sample size of $n = 10$ and a significance level of 5%.

It can also be concluded from the correlation test that the assumption of multivariate normality is tenable at 5% level of significance.

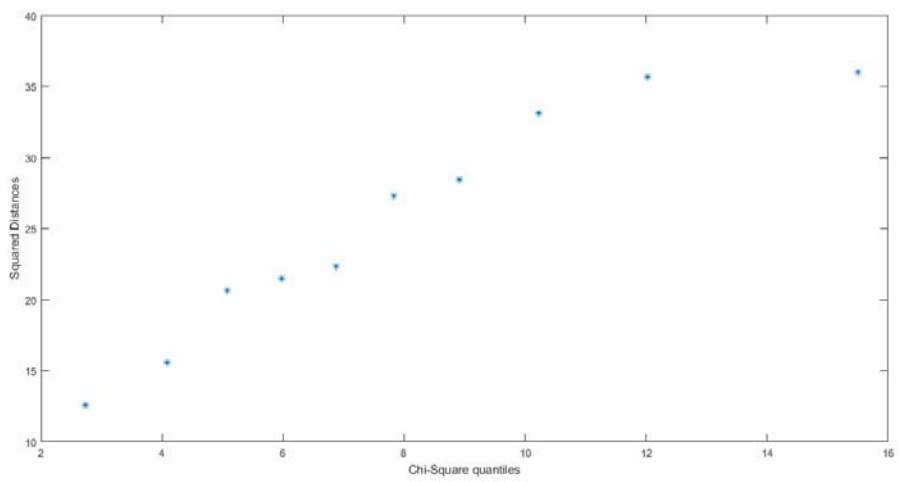

Figure 6. Chi-square plot.

3.1. Results from repeated measures design

The independence of observations (or, more precisely, independent and identically distributed variables) assumption is often satisfied when observations are captured from different individuals. In this study, the recognition distances were captured for different individuals. Table 1 shows the multivariate tests.

Table 1. Multivariate tests

Effect	Value	*F*	Hypothesis df	Error df	Sig.
Pillai's trace	0.987	31.543	7.000	3.000	0.008
Wilks' lambda	0.013	31.543	7.000	3.000	0.008
Hotelling's trace	73.600	31.543	7.000	3.000	0.008
Roy's largest root	73.600	31.543	7.000	3.000	0.008

From Table 1, the null hypothesis of equality of average recognition distance is not tenable since the Hotelling trace *p*-value (0.008) is less than 0.05 level of significance. The other test statistic presented in Table 1 has *p*-values that are same as Hotelling trace.

Table 2 shows the Mauchly's test of sphericity. The null hypothesis of this test is given as: the covariance matrix of the orthonormalized

transformed dependent variables is proportional to an identity matrix. This means that the population variances of all recognition distances for the specified constraints are equal.

Table 2. Mauchly's test of sphericity

Mauchly's *W*	Approx. Chi-square	df	Sig.	Greenhouse-Geisser	Huynh-Feldt	Lower-bound
0.000	217.030	27	0.000	0.158	0.163	0.143

From Table 2, the assumption of homogeneity of variance within-subjects is violated since the *p*-value of the Mauchly's *W* (0.000) is less than 0.05 level of significance. Greenhouse Geisser, Huynh-Feldt or lower-bound were used to estimate the amount of sphericity. If sphericity is violated, then the aforementioned methods are used to correct the within-subjects tests.

Table 3. Test of within-subjects effects

Source	Type III sum of squares	df	Mean square	*F*	Sig.
Sphericity assumed	10933.357	7	1561.908	76.707	0.000
Greenhouse-Geisser	10933.357	1.103	9913.066	76.707	0.000
Huynh-Feldt	10933.357	1.143	9562.441	76.707	0.000
Lower-bound	10933.357	1.000	10933.357	76.707	0.000

From Table 3, the Greenhouse-Geisser correction is robust to the violation of the sphericity assumption. The Greenhouse-Geisser test's *p*-value (0.000) is less than 0.05 level of significance. It can therefore be concluded that there exists a significant difference between the average recognition distance of the various head-poses from their straight-pose when the study algorithm is used for recognition.

Table 4 shows that there is no significant difference between head-poses (4° and 8°), (8° and 12°), (12° and 16°), (16° and 20°), (20° and 24°), (24° and 28°) and (28° and 32°) in the average recognition distance from the straight-pose (0°) when the study algorithm (FFT-PCA/SVD) is used for recognition.

Thus there is no significant difference between head-poses in the average recognition distance from the straight-pose (0°) for constraints with 4° difference.

It is evident from Table 4 that a significant difference exists in average recognition distances of the remaining constraints at 5% level of significance. It can also be seen from the estimated mean difference that the recognition distances of the various angular constraints (4°, 8°, 12°, 16°, 20°, 24°, 28° and 32°) from their straight-pose (0°) increase with increasing head-pose.

Table 4. Pairwise comparisons

	4°	8°	12°	16°	20°	24°	28°
8°	5.79						
12°	11.34∗	5.56					
16°	16.89∗	11.11∗	5.55				
20°	22.26∗	16.47∗	10.91∗	5.37			
24°	27.33∗	21.54∗	15.98∗	10.43∗	5.07		
28°	31.91∗	26.12∗	20.56∗	15.01∗	9.65∗	4.58	
32°	34.77∗	28.98∗	23.42∗	17.87∗	12.51∗	7.44∗	2.86

Significant codes: less than 0.05 "∗"

3.2. Numerical evaluations

The methods adopted for numerical assessment in this study were average recognition rate and the computational time. According to Asiedu et al. [1], recognition rate of an algorithm is defined as the ratio of the total number of correct recognitions by the algorithm to the total number of images in the test set for a single experimental run. Recognition performance has many measurement standards. The average recognition rate, R_{avg}, of an algorithm is defined as

$$R_{avg} = \frac{\sum_{i=1}^{t_{run}} n_{cr}^{i}}{t_{run} \times n_{tot}}, \tag{2.12}$$

where t_{run} is the number of experimental runs. The n_{cr}^{i} is the number of

correct recognitions in the *i*th run and n_{tot} is the total number of faces being tested in each run. The average error rate, E_{avg}, is defined as $100 - R_{avg}$.

The total number of correct recognitions $\sum_{i=1}^{20} n_{cr}^{i}$, for the study of algorithm is 74.

The total number of experimental runs, $t_{run} = 20$.

The total number of images in a single experimental run, $n_{tot} = 4$.

Hence, the average recognition rate of study algorithm (FFT-PCA/SVD)

$$R_{avg} = \frac{74}{(20)(4)} \times 100$$

$$= 92.5\%.$$

The average error rate

$$E_{avg} = 100 - R_{avg}$$

$$= 100 - 92.5$$

$$= 7.5\%$$

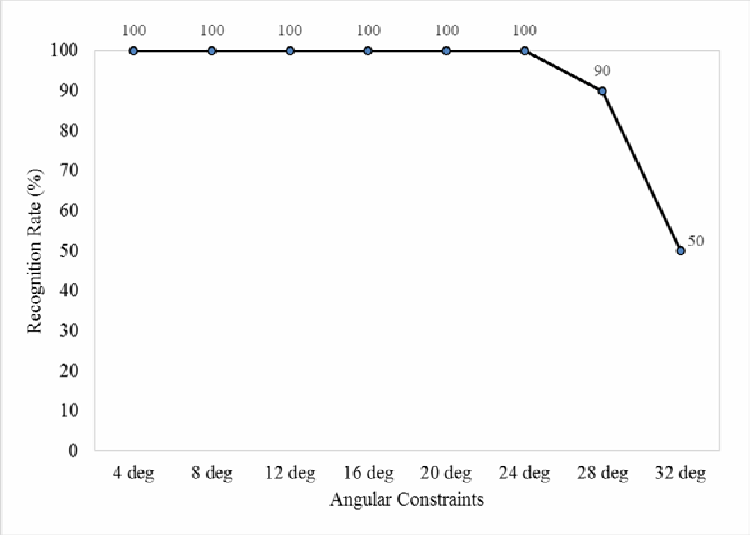

Figure 7. A graph of recognition rates against the various constraints.

It can be seen from Figure 7 that there is a perfect recognition (100%) for angular constraints (4° to 24°) but the recognition rate declined for constraints above 24°. This means that when FFT-PCA/SVD is used for recognition of face images under angular constraints, the recognition rate decreases for head poses greater than 24°.

The average runtime of the study algorithm in the recognition of the 80 test images was approximately 4 seconds.

4. Conclusion

The study sought to investigate whether a significant difference exists in the average recognition distance of the specified angular constraints (4°, 8°, 12°, 16°, 20°, 24°, 28° and 32°) from their straight-pose (0°) when being recognized by FFT-PCA/SVD algorithm. It was found that there were no statistical significant differences in average recognition distances for head-poses with 4° difference.

The findings of the study also revealed that the study algorithm (FFT-PCA/SVD) recognizes perfectly (100% recognition rate) head-poses that are 24° and below. The average recognition rate for the study algorithm (FFT-PCA/SVD) was found to be 92.5% with an error rate of 7.5% on the adopted study database. It can therefore be inferred that FFT-PCA/SVD has an appreciable performance when used to recognize face images under angular constraints. The algorithm's (FFT-PCA/SVD) average computational time in the recognition of all 80 test images was approximately 4 seconds.

5. Recommendations

FFT-PCA/SVD recognition algorithm performed creditably well under angular constraints. It is therefore recommended that the study algorithm (FFT-PCA/SVD) be adopted in application areas that have head-poses as constraints.

The study algorithm's performance (recognition rate) declined to 90% and 50% for head-poses 28° and 32°, respectively. Future study should be

targeted at modifying the algorithm to improve its performance as the degree of head-tilt increases.

It is also recommended that the performance of FFT-PCA/SVD be assessed on other constraints such as ageing, occlusions, face image in glasses, and lightening conditions.

Acknowledgement

The authors are thankful to Carnegie Next Generation of Africa Academics, who through Banga-Africa write-shop supported this manuscript.

References

[1] L. Asiedu, A. O. Adebanji, F. Oduro and F. O. Mettle, Statistical evaluation of face recognition techniques under variable environmental constraints, International Journal of Statistics and Probability 4(4) (2015a), 93-111.

[2] L. Asiedu, A. O. Adebanji, F. Oduro and F. O. Mettle, Statistical assessment of PCA/SVD and FFT-PCA/SVD under varying facial expressions, British Journal of Mathematics and Computer Science 12(6) (2015b), 1-23.

[3] J. A. Doornik and H. Hansen, An Omnibus test for univariate and multivariate normality, Oxford Bulletin of Economics and Statistics 70 (2008), 927-939.

[4] E. F. Glynn, Fourier Analysis and Image Processing, Stowers Institute for Medical Research, 2007.

[5] R. A. Horn and C. R. Johnson, Topics in Matrix Analysis, Cambridge University Press, New York, 1991.

[6] M. Kirby and L. Sirovich, Application of the Karhunen-Loéve procedure for the characterization of human faces, IEEE Trans. Pattern Analysis and Machine Intelligence 12(1) (1990), 103-108.

[7] S. M. Lajevardi and Z. M. Hussain, Novel higher-order local autocorrelation-like feature extraction methodology for facial expression recognition, IET Image Process 4 (2010), 114-119.

[8] D. Morrigan, S. Arumugam, K. Rajalakshmi and T. Manish, Performance evaluation of face recognition using Gabor filter, log Gabor filter and discrete wavelet transform, International Journal of Computer Science and Information Technology 2(1) (2010), 125-133.

[9] D. Samal and V. Starovoitov, Approaches and methods to face recognition. A survey, Institute of Engineering Cybernetics, 8, Minsk, 1998, 54 pp.

[10] J. Shlens, A Tutorial on Principal Component Analysis, Derivation, Discussion and Singular Value Decomposition, Version 1, Princeton, USA, 2003, pp. 1-15.

[11] M. Turk and A. Pentland, Eigenface recognition, Journal of Cognitive Neuroscience 3(1) (1991), 71-86.

[12] P. Wagner, Face recognition with python, 2012.
Retrieved from: http://www.bytefish.de

[13] B. Weyrauch, J. Huang, B. Heisele and V. Blanz, Component-based face recognition with 3D morphable models, First IEEE Workshop on Face Processing in Video, Washington, DC, 2004.

Appendix 1.0

Appendix 1.0 contains the 8-variates recognition distances (distance between the specified head-poses from their straight-pose (0°)) used for the statistical assessment of the study algorithm.

Appendix 1.0. Recognition distance from FFT-PCA/SVD

Subject	4°	8°	12°	16°	20°	24°	28°	32°
1	6.4443	12.549	18.168	23.378	7.844	31.701	35.220	35.949
2	4.4414	10.076	15.876	22.391	28.646	35.618	42.119	48.482
3	4.3553	9.400	13.538	17.704	22.290	27.102	32.069	37.282
4	5.2552	9.1987	12.778	16.498	19.351	21.447	23.210	24.929
5	3.0838	6.7859	10.124	13.448	16.810	20.324	23.814	27.004
6	4.9905	10.953	16.750	21.843	27.048	31.356	35.068	35.306
7	5.6938	11.289	17.016	22.753	28.061	32.712	37.098	40.486
8	5.9992	12.095	17.701	22.625	26.747	30.066	32.485	30.894
9	6.3476	14.544	22.222	30.575	39.372	47.930	54.955	61.346
10	5.0754	12.674	20.950	29.404	38.097	46.683	54.701	57.684